

Article

Erosion Wear Investigation of HVOF Sprayed WC-₁₀Co₄Cr Coating on Slurry Pipeline Materials

Kaushal Kumar ^{1,*}, Satish Kumar ², Gurprit Singh ², Jatinder Pal Singh ² and Jashanpreet Singh ²

¹ Department of Mechanical Engineering; Guru Jambheshwar University of Science & Technology, Hisar 125001, India

² Department of Mechanical Engineering; Thapar University, Patiala 147004, India; satish.kumar@thapar.edu (S.K.); gurprit.singh@thapar.edu (G.S.); jatinderpal.singh@thapar.edu (J.P.S.); jashanpreet.singh@thapar.edu (J.S.)

* Correspondence: ghanghaskaushal@gmail.com; Tel.: +91-981-282-0004

Academic Editor: James Kit-hon Tsoi

Received: 19 February 2017; Accepted: 29 March 2017; Published: 12 April 2017

Abstract: In the present work, erosion wear due to slurry mixture flow has been investigated using a slurry erosion pot tester. Erosion tests are conducted on three different slurry pipe materials, namely, mild steel, SS202, and SS304, to establish the influence of rotational speed, concentration, and time period. In order to increase erosion wear resistance, a high-velocity oxy-fuel (HVOF) coating technique is used to deposit a WC-₁₀Co₄Cr coating on the surface of all piping materials. Experimental results show that rotational speed is a highly-influencing parameter for the erosion wear rate as compared to solid concentration, time duration, and weighted mean diameter. WC-₁₀Co₄Cr HVOF coating improved the erosion resistance of piping materials up to 3.5 times. From experimental data, the exponents of solid concentration, velocity, and the size of particles are calculated for the empirical erosion wear equation. A functional equation of the erosion wear rate is developed. The predicted erosion wear is in agreement with the experimental data and found to be within a deviation of ±12%.

Keywords: erosion wear; bottom ash; slurry pipe materials; powder coating

1. Introduction

Slurry pipelines are used in various industrial applications, such as disposal of waste material, coal ash, and tailing materials [1]. However, knowledge, as well as technology, associated with the design and operation of such pipelines is still developing. Thus, many aspects of the design have to be done with the help of semi-empirical correlations based on experimental data. This is due to large number of variable factors involved in the design [2–4]. Accurate prediction of erosion wear rate is very important for the slurry pipeline [5,6]. Over the years, various bench scale setups have been developed to simulate the erosion wear mechanism at the laboratory scale [3,4]. Various researchers have found that particle size distribution, rotational speed, and solid concentration are the major factors that influence the material's erosion wear rate [7–9]. Some investigators have suggested that the erosion wear can be minimizing by using protective coatings on piping materials. These coatings can provide a hard layer of carbides, oxides, and nitrides of Cr, W, Al, and Ti [10,11]. The high-velocity oxy-fuel (HVOF) technique can be applied to deposit coatings with high cohesive strength and superior mechanical properties [10–14]. In the present work, erosion wear behavior of three piping materials, namely, mild steel, SS202, and SS304, have been analyzed with and without a HVOF-sprayed WC-₁₀Co₄Cr coating. The present study is conducted with the motivation of measuring the average erosion wear at specimen placed in horizontal direction. The erodent material is taken as bottom ash having a solid concentration that varies from 30 wt % to 60 wt %. Experiments are carried out at four different speeds, namely, 600, 900, 1200, and 1500 rpm with time durations of 90, 120, 150, and 180 min.

2. Material and Methods

2.1. Specimen

For the study of erosion wear, the base material is cut into flat pieces of 75 mm × 25 mm × 5 mm and each drilled with a central hole for holding purposes in the rotating spindle of the tester. Chemical composition of the base material is measured by using an optical emission spectrometer (Foundry Master, Oxford instruments, Udem, Germany). The optical emission spectrometer was installed to ensure the precise chemical composition of ferrous metals. The surface roughness of specimen is determined by using a roughness tester (Model SJ400, Surf test, Mitutoyo America Corporation, CA, USA) with a lowest count of 0.001 mg. The mean roughness values are determined before and after erosion wear experimentation. The mean hardness of all coated and uncoated specimens are determined by using a micro Vicker hardness tester (Model MVH1, Metatech Industries, Pune, India) with a load of 1000 g. The microhardness was tested at four different spots on the specimen's surface by the Vicker's diamond pyramid at regular separation distances. The purpose of regular indentation was to avoid cracking of the specimen under the applied load (by the indenter).

2.2. Coating Deposition

Commercially available coating powder WC₁₀Co₄Cr has been used in the present study to provide resistance against slurry erosion. Energy-dispersive spectroscopy (EDS) analysis of the coating powder confirms the presence of different elements in the powder. A high velocity oxy-fuel technique is used to deposit the coating on piping materials by applying the HIPOJET 2700 (M/S Metalizing Equipment Company Private Limited, Jodhpur, Rajasthan, India) thermal spray process. A compressed air jet is used for cooling the test specimens during and after the coating process. The process variables used for the thermal spray process are listed in Table 1. Prior to powder coating deposition, the surface of steel specimens are grit-blasted with Al₂O₃ grit, which increases the quality of coating adhesion by enhancing the surface roughness of the specimens.

Table 1. The process variables for the thermal spray process.

Medium	Spray Distance (mm)	Flow Rate (L/min)	Pressure (kPa)	Feed Rate (g/min)	Particle Size (μm)
Air	138	640	10	30	15
Oxygen	138	260	5	30	15
Fuel	138	75	6.2	30	15

2.3. Slurry Preparation

The erodent material is taken as bottom ash, evacuated from the Rajiv Gandhi thermal power plant (Hisar, Haryana, India). The particle size distribution (PSD) of bottom ash sample is evaluated with the help of standard sieves. The solid concentration of the slurry varied from 30 wt % to 60 wt %. The specific gravity of the bottom ash sample is measured by using pycnometer equipment. The static settled concentration value is determined by preparing a solid-liquid suspension of an initial solid concentration, i.e., 30 wt %. The surface morphology and composition of the bottom ash is measured by using scanning electron microscopy (SEM) and energy dispersive X-ray spectroscopy (EDX) (Model JSM-6510LV, JOEL Ltd., Nieuw-Vennep, The Netherlands).

2.4. Slurry Erosion Test Rig

Slurry erosion wear tests are performed with the help of an erosion pot tester with 1.8 L capacity (model: TR-41, Ducom instruments, Bangalore, India) in a similar approach as adopted by [8]. The schematic diagram of the test rig is shown in Figure 1. The tester consists of a rotating spindle, cylindrical pot, propeller, and screw jack. The rotating spindle, itself, holds the specimen and propeller

fixed to it. With the rotation of the spindle, the specimen and propeller also rotate. A propeller is fixed at the end of the spindle so that slurry particles do not settle but remain suspended in the mixture throughout the working process. A proximity sensor disc is used to measure the speed of the spindle. Specimens were washed with acetone after each test run. An electronic weight microbalance is used to calculate the weight loss of specimens with 0.001 mg resolution.

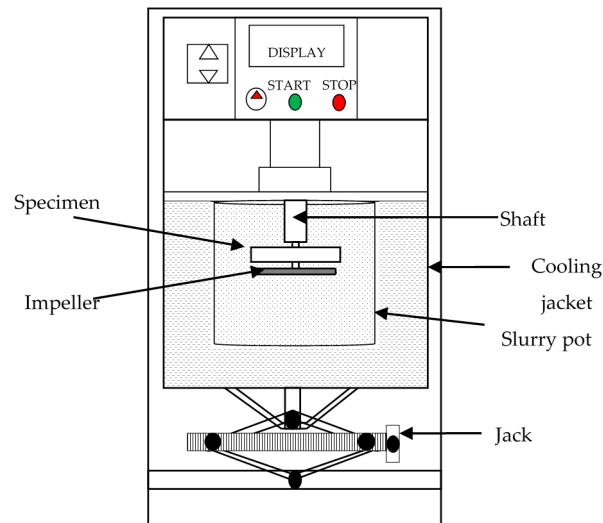


Figure 1. Schematic diagram of the erosion wear pot tester used for the investigation.

3. Results and Discussion

3.1. Characterization of Erodent Material

Bottom ash was used as the erodent material to perform the erosion wear experiments. The surface morphology of the bottom ash sample is shown in Figure 2a. It seems that particles of bottom ash are coarser, asymmetrical, darker grey in color due to the existence of unburned carbon, and have an uneven surface texture. The chemical composition of the bottom ash sample is shown in Figure 2b. The chemical composition of the bottom ash sample is expressed as follows: SiO₂-52.11 wt %, Al₂O₃-36.24 wt %, FeO-2.15 wt %, TiO₂-1.68 wt %, CaO-1.28 wt %, CO₂-3.19 wt %, and LOI-3.35 wt %.

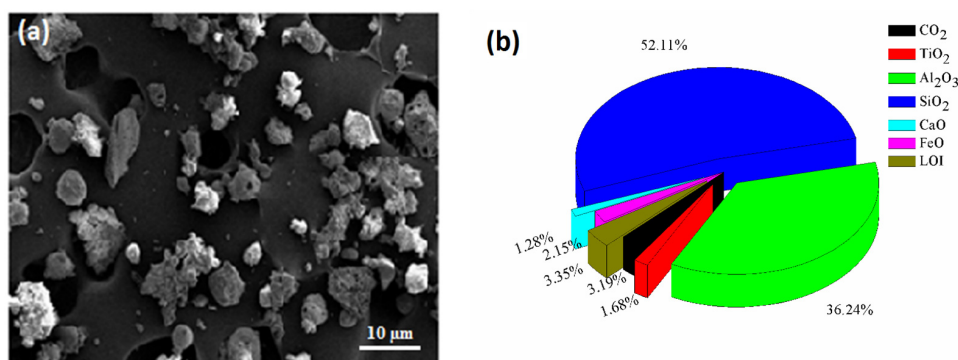


Figure 2. (a) SEM morphology and (b) chemical composition of bottom ash sample.

Figure 3 represents the particle size distribution (PSD) of the bottom ash sample. It was observed that more than 19.41% particles are coarser than 250 μm, 65.20% particles are in the range of 75–250 μm, and only 15.39% particles are finer than 75 μm. The specific gravity of the bottom ash sample was measured as 1.94. Table 2 represents the final static settled concentration of the slurry suspension, which was recorded as 52.15 wt %.

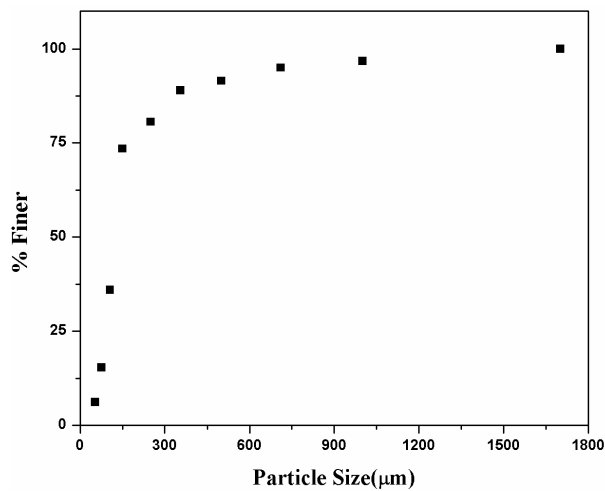


Figure 3. Particle size distribution (PSD) of bottom ash.

Table 2. Static settled concentration of bottom ash (wt %).

Time (min)	Static Settled Concentration (wt %)	Time (min)	Static Settled Concentration (wt %)
0	30	20	37.75
1	30.12	30	41.05
2	30.35	60	45.73
3	30.72	180	49.92
4	31.16	420	51.36
5	31.95	660	52.15
10	34.92	–	–

3.2. Effect of WC₁₀Co₄Cr Coating Powder Deposition on Substrate

The morphology of the coating powder is studied by performing scanning electron microscopy, as shown in Figure 4. It is observed that the coating powder has an angular morphology. The coatings, with thicknesses in the range of 166–175 μm, were deposited on the surfaces of the substrates. The chemical compositions of the base materials were measured by using an optical emission spectrometer, summarized in Table 3. The percentage of Ni and Cr was found to be at their maxima in SS304, whereas Mn was found to be at its maximum in SS202. The percentage of Ni, Cr, and Mn were found highest in SS202, which is beneficial in providing better microhardness. The average microhardness and roughness of uncoated and WC₁₀Co₄Cr-coated materials is presented in Table 4. From Table 4, it seems that SS202 has better hardness and roughness as compared to mild steel and SS304. However, the roughness of SS202 was increased approximately three times with the deposition of WC₁₀Co₄Cr coating powder.

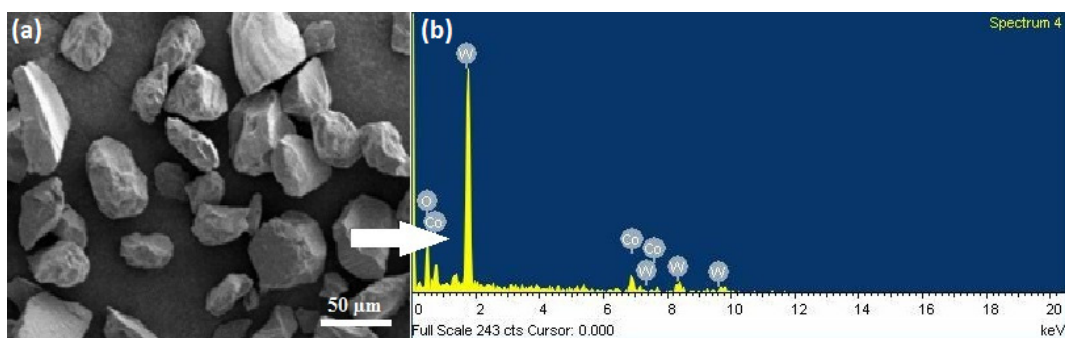


Figure 4. (a) SEM and (b) EDS micrographs of WC₁₀Co₄Cr coating powder.

Table 3. Chemical composition of base materials (wt %).

Material	Fe	Cr	Ni	Mn	C	Si	Co	P	Al	S	Cu
Mild Steel	98.90	0.04	0.05	0.45	0.14	0.20	–	0.07	0.02	0.06	0.07
SS202	74.54	13.42	0.18	9.67	0.09	0.42	0.05	0.07	0.04	0.04	1.48
SS304	69.65	18.65	8.94	1.43	0.13	0.55	0.18	0.11	–	0.06	0.30

Table 4. Effect of WC-₁₀Co₄Cr coating on different properties of piping materials.

Materials	Indentation Depth (μm)		Average Hardness (HV)		Average Roughness (μm)	
	Uncoated	Coated	Uncoated	Coated	Uncoated	Coated
Mild steel	103	37	138	952	2.23	5.48
SS202	82	25	276	1158	1.63	5.81
SS304	96	29	237	1129	1.56	5.78

3.3. Effect of Rotational Speed/Velocity on Average Erosion Wear

Many researchers have found that rotational speed, solid concentration and particle size distribution are some of the major factors that influence the erosion wear rate [4,15,16]. The following empirical correlation has been used to predict the erosion wear by using experimental data, and has also been discussed [15].

$$E_w = kv^a d_e^b C_w^c \quad (1)$$

where E_w is the erosion rate, v is the velocity, d_e is the particle size, C_w is the solid concentration of slurry, and four constants k , a , b , and c . The regression analysis is carried out to find the value of exponents “ a ”, “ b ”, and “ c ” [17]. In the present work, erosion wear on the different piping materials has been investigated with and without coating to study the influence of three different parameters, namely, the speed of rotation, solid concentration, and test duration. The values of exponent “ a ” have been determined as 2.06, 1.53, and 1.69 for mild steel, SS202, and SS304, respectively, which shows good agreement with researchers [2,15]. Truscott [18] reported that value of the velocity exponent lies between 1 and 3.5. Values of $a < 2$ (1.53 and 1.69) represent that the bottom ash particles rebound from the surface of SS202 and SS304 at high impact velocity. However, $a = 2.06$ represents that erosion wear approaches the ideal value, which is directly proportional to the kinetic energy of the impacting particles. The erosion wear experimentation performed at four different rotational speeds of 600, 900, 1200 and 1500 rpm with a time duration of 180 min, and a solid concentration of 30 wt %. The erosion wear of piping material is evaluated in the terms of the cumulative weight loss per unit surface area of the test specimen (g/m^2). The linear speed on the surface of the specimen increases with the rotation radius, thus, the erosion wear of the specimen is average. The effect of the rotational speed on the average erosion wear of coated and uncoated piping materials is shown in Figure 5a.

It has been observed that uncoated SS202 and SS304 exhibit higher erosive resistances as compared to mild steel at all speeds. The order of decreasing erosion wear was found to be mild steel > SS304 > SS202. Results indicated that when the rotational speed increases from 600 to 1500 rpm, erosion wear increases to about 107%, 87.41%, and 90.41% for mild steel, SS202, and SS304, respectively. Hence, it is clear that erosion wear shows high dependence on rotational speed. The kinetic energy of erodent particles increases with rotational speed. This increase in kinetic energy will lead to more localized attacks at several spots on the target material and can cause severe plastic deformation, which leads to more erosion wear. It has also been realized that the mild steel specimen exhibits higher erosion wear rather than SS202 and SS304 specimens at all rotational speed. This is anticipated due to much harder nature of SS202 and SS304 as compared to mild steel. Experimental data shows good agreement with the findings of [2,11,15].

3.4. Effects of Solid Concentration on Average Erosion Wear

The erosion wear rate of different piping materials at a concentration range of 30%–60%, at a speed of 600 rpm, for 180 min test run duration, is shown in Figure 5b. It has been observed that

erosion wear increases nonlinearly with the increase in the solid concentration of bottom ash slurry. From the experimental results it has been concluded that erosion wear increases by 53.63% for mild steel, 41.72% for SS202, and 45.33% for SS304 when the solid concentration increases from 30 wt % to 60 wt %. The amount of solid particles per unit volume increases due to increases in the solid concentration of the slurry. Therefore, higher concentration allows a larger number of solid particles to strike on the surface of the wear specimen, which tends to increase the erosion wear of the material. Similar observations have also been made by other researchers with fly ash and sand slurry [4,6]. The value of exponent “ c ” for mild steel, SS202, and SS304 was determined as 0.642, 0.515, and 0.537, respectively, for Equation (1). The value of the exponents for all three uncoated piping materials show better agreement with researchers [15].

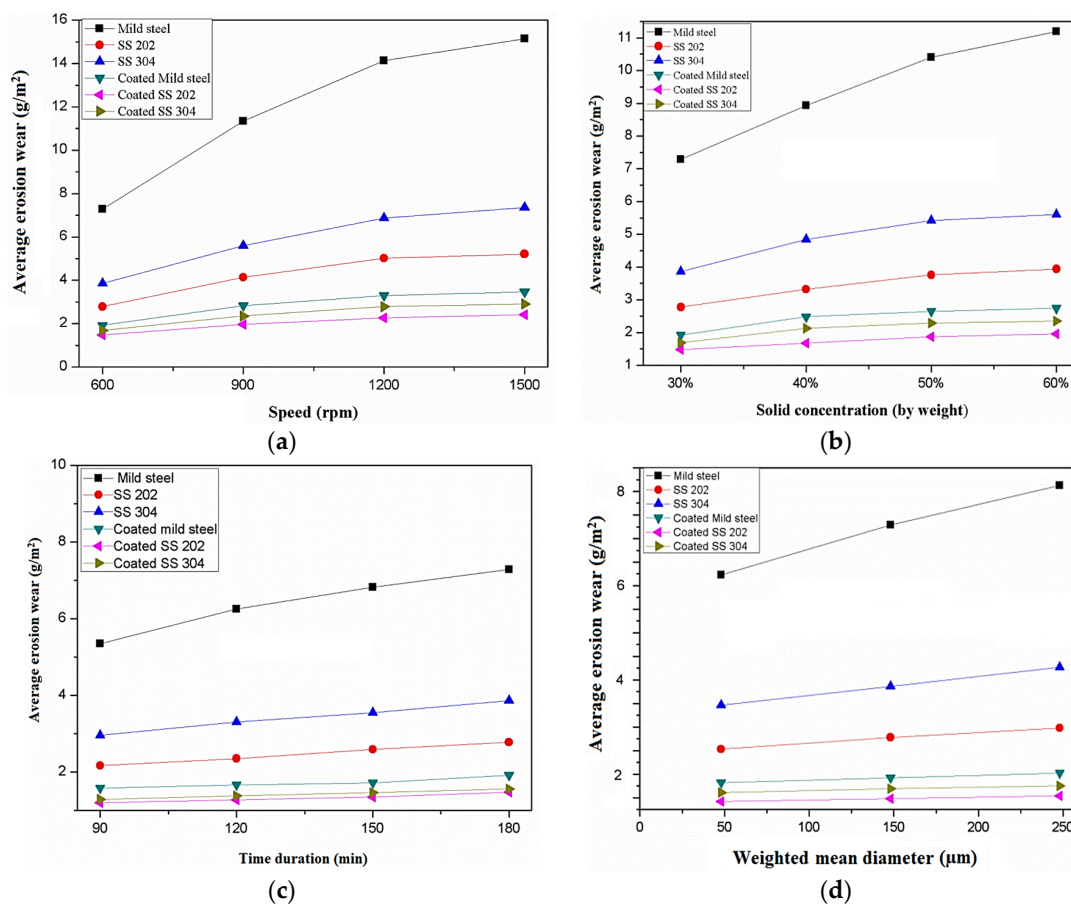


Figure 5. Effect of rotational speed on average erosion wear of uncoated and coated steel (a) for $C_w = 30\%$ and time = 180 min; (b) speed = 600 rpm and time = 180 min; (c) speed = 600 rpm and $C_w = 30\%$ and (d) speed = 600 rpm, $C_w = 30\%$ and time = 180 min.

3.5. Effects of Time Duration on Average Erosion Wear

The effect of time duration on the erosion wear performance of piping materials, with and without coating, was also examined. The erosion wear experiments were performed at four different time durations: 90, 120, 150 and 180 min, at a rotational speed of 600 rpm and solid concentration of 30 wt %, which is shown in Figure 5c. The erosion wear of different piping materials, namely, mild steel, SS202, and SS304, increases with time variation for coated and uncoated steels [15]. It has been concluded from the above results that, with the increase in time duration, the erosion wear of mild steel, SS202, and SS304 increases by 36.26%, 28.11% and 30.40%, respectively. This can be due to the fact that the continuous impinging action of the erodent on the target surface results in higher erosion wear. Similar trends were reported by the authors [4,11,15].

3.6. Effect of Weighted Mean Diameter on Average Erosion Wear

The effect of mean particle diameter on erosion wear was studied for both uncoated and coated piping materials, as shown in Figure 5d. The researchers concluded that the weighted mean diameter of multi particulate slurry is the most appropriate parameter as compared to d_{50} and the median diameter (arithmetic mean of the particle diameter) [15]. In the present investigation the weighted mean diameter was taken as 48, 148 and 248 μm .

From Figure 5d, it is seen that erosion wear increases with the increase in particle size for all materials, whether coated or uncoated. In other words, the finer particles show less erosion wear as compared to coarser particles. With an increase in the particle size of the erodent, the kinetic energy of the impact particles increases, which is further responsible for increases in the erosion wear. Additionally, in the present study, specimens are fixed in the horizontal direction and impingement angles are very low, i.e., approaches to 0° . Thus, mild steel shows the rebounding of particles as compared to SS202 and SS304. The values of exponent "b" are determined as 0.414, 0.295 and 0.316, respectively, for mild steel, SS202, and SS304 for Equation (1). The values of exponent "b" show good agreement with researchers [2,15,19]. The value of exponent "a" is much higher as compared to exponent "b". The results show that rotational speed exhibits a highly-influencing parameter as compared to particle size and solid concentration.

3.7. Effect of WC-10Co4Cr Coating on Average Erosion Wear

To study the effect of coating WC-10Co4Cr on piping materials of mild steel, SS202, and SS304, the erosion wear experiments were performed at different rotational speeds, solid concentrations, and time durations, which are shown in Figure 5a–d. Experimental results indicated that coated mild steel, SS202 and SS304 exhibit high slurry erosive wear resistance as compared to uncoated materials. However, the trend of increasing wear is nonlinear throughout the entire experiment. Nevertheless, a remarkable resistance in erosion wear has been observed after WC-10Co4Cr coating for all three piping materials. It is worth noting that coated specimens followed a similar trend as uncoated specimens in the case of increasing wear rate, i.e., mild steel > SS304 > SS202. The coated mild steel reported higher erosion wear than coated SS202 and SS304 for all sets of parameters. The coated SS202 shows the least erosion wear at 30% concentration with 600 rpm for 90 min as compared to mild steel and SS304. After WC-10Co4Cr coating, it was clear that the erosion resistance of mild steel improved in the range of 2.5 to 3.5 times, whereas in SS202 and SS304 improved nearly 1.5 to 2.3 times. Furthermore, it can be also concluded that the rate of increase in erosion wear of coated and uncoated materials also resulted from the increase in variable parameters. The value of exponent "a" was determined as 1.21, 1.14, and 1.16 for coated mild steel, SS202, and SS304, respectively, which shows good agreement with researchers [2,15]. A value of $a < 2$ represents that the bottom ash particles rebound from the specimen surface at high impact velocity. Moreover, the value of exponent "a" drops after deposition of WC-10Co4Cr powder. This indicates that WC-10Co4Cr coating adds to the brittle nature of ductile stainless steels.

3.8. Visual Examination of Eroded Coated Surfaces

Scanning electron microscopy (SEM) of eroded surfaces is used to study the surface morphology of coated specimens. After the erosion experimentation the specimen undergoes roughness and hardness testing again. It was observed that the roughness of the entire specimens decreases, whereas no change in harness is observed. The average roughness of uncoated mild steel, SS202, and SS304 is observed as 2.45, 1.35, and 1.38 μm , whereas the values were 4.89, 4.63, and 4.58 μm after deposit coating. The investigators suggested that cutting, fracture, and abrasion are the major modes of erosion wear mechanisms that are relevant to slurry pipelines [2,3,13,14]. The eroded images of WC-10Co4Cr-coated mild steel, SS202, and SS304 with EDS (energy dispersive spectroscopy) are shown in Figures 6–8. It has been observed that the tungsten carbide phase is visualized in more areas on the surface of the SS202 substrate as compared to mild steel and SS304. From Figures 6 and 7, it is noticed that mild steel was eroded more

than SS202; this may be due to less affinity of mild steel towards tungsten-based coatings as compared SS202, since less tungsten carbide phases were detected on the surface of coated mild steel substrate. A small amount of erodent was also found in SEM micrographs on the surface of materials, which may be due to embedment of hard erodent particles in the relatively soft Co matrix. A long peak of tungsten confirms its existence in the dark phase of the topography. The presence of wear marks can be observed on the worn surface caused by micro-cutting, carbide-fracture, and lip formation. It has been stated that surface wear occurring through micro-cratering is responsible for material removal.

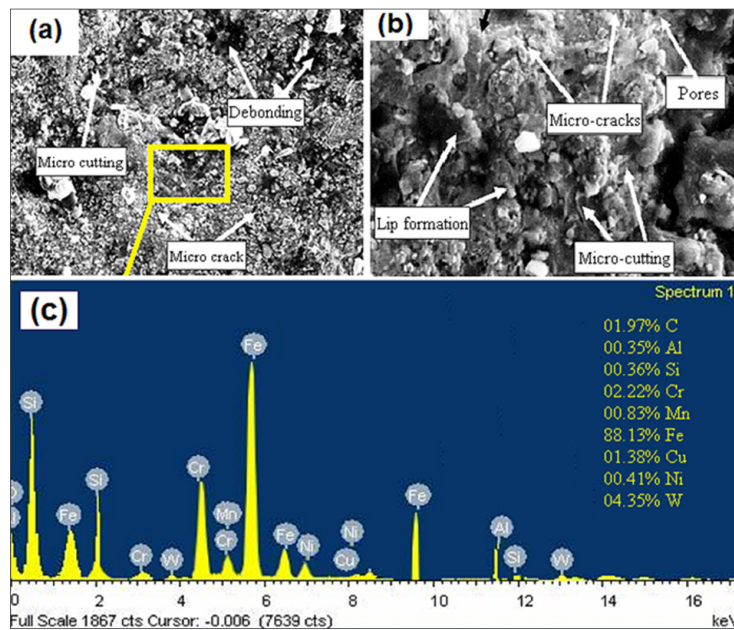


Figure 6. Eroded surface morphology of WC-10Co4Cr coated mild steel: SEM micrographs at (a) 1000×, (b) 100× magnification and (c) EDS micrographs.

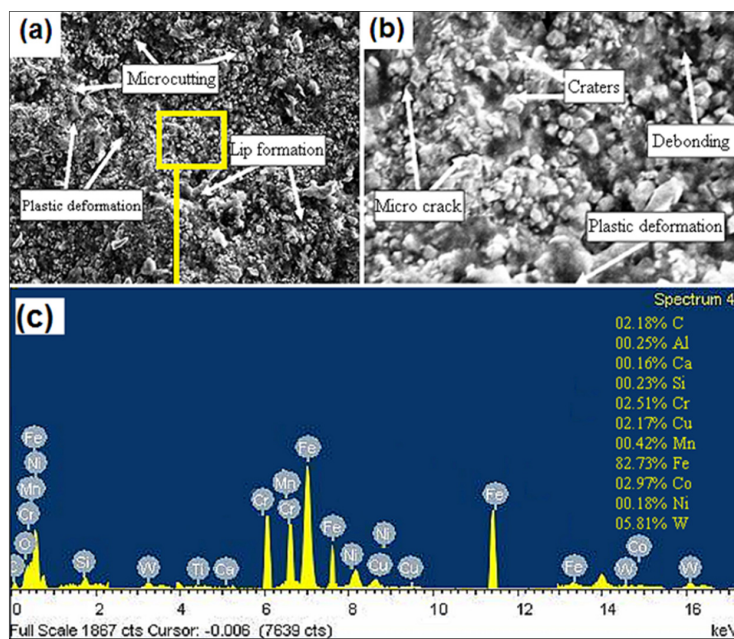


Figure 7. Eroded surface morphology of WC-10Co4Cr coated SS202: SEM micrographs at (a) 1000×, (b) 100× magnification and (c) EDS micrographs.

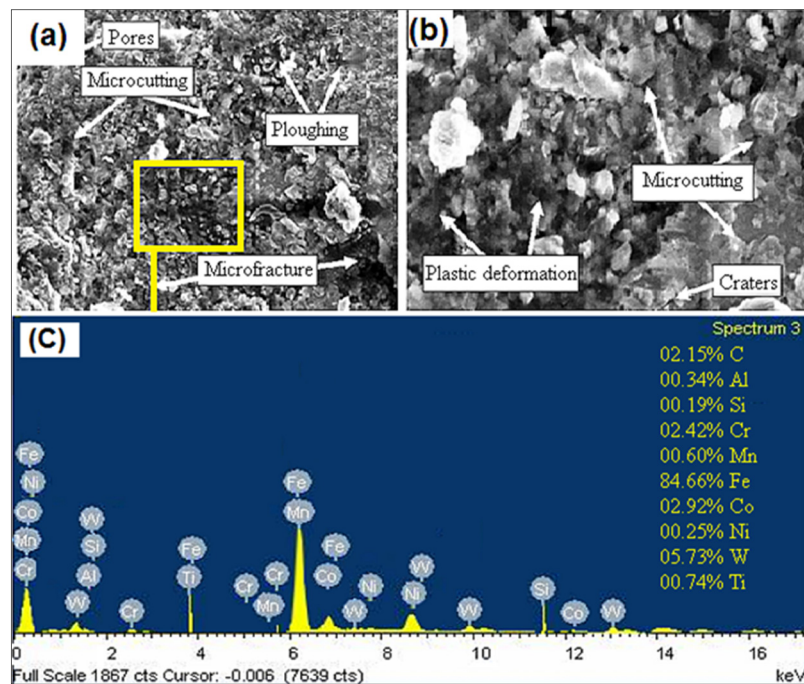


Figure 8. Eroded surface morphology of WC₁₀Co₄Cr coated SS304: SEM micrographs at (a) 1000×, (b) 100× magnification and (c) EDS micrographs.

3.9. Correlation for Erosion Wear

The effects of velocity, solid concentration, and particle size on erosion wear of piping materials, namely, mild steel, SS202 and SS304, are analyzed. An attempt has been made to develop a correlation to estimate the erosion wear in terms of weight loss ($\text{mm}\cdot\text{year}^{-1}$) as given below:

$$E_Y = \frac{W_L}{S \times A} \times \frac{8760}{T} \times 10^3 \quad (2)$$

where W_L is the measured weight loss (kg), A is the surface area, S is the density of pipe material and T is the duration of test (h).

Extensive experimentation was performed to determine the functional relationship of dependent parameters, like solid concentration, velocity, and particle size, on the erosion wear. The weighted mean diameter of bottom ash is calculated as 48, 148 and 248 μm . A total of 48 data points were generated for each material. Initially, the erosion wear variation of bottom ash slurry with solid concentration, velocity, and particle size for mild steel, SS202 and SS304 are plotted on log-log graphs to obtain the functional relationship between them.

Equation (1) of erosion wear for mild steel, SS202 and SS304 can be written as:

$$E_{Y \text{ MS}} = 0.211v^{2.06}d_e^{0.414}C_w^{0.642} \quad (3)$$

$$E_{Y \text{ SS202}} = 0.27v^{1.53}d_e^{0.295}C_w^{0.515} \quad (4)$$

$$E_{Y \text{ SS304}} = 0.223v^{1.69}d_e^{1.69}C_w^{0.537} \quad (5)$$

The predicted erosion wear is calculated from the abovementioned correlation. To achieve better precision, actual experimental values of erosion wear have been compared to the predicted values obtained from correlations. Figure 9 shows the variation of erosion wear for experimental and theoretical values obtained with 48 data points for mild steel, SS202 and SS304. Predicted erosion wear values ideally match with experimental values at the 45° line. A reasonable agreement has been

observed. It is observed that erosion wear was found within the deviation limits from $\pm 12\%$, $\pm 9\%$ and $\pm 8\%$ for mild steel, SS304 and SS202, respectively. This deviation range was found to be acceptable by researchers [2,3,15].

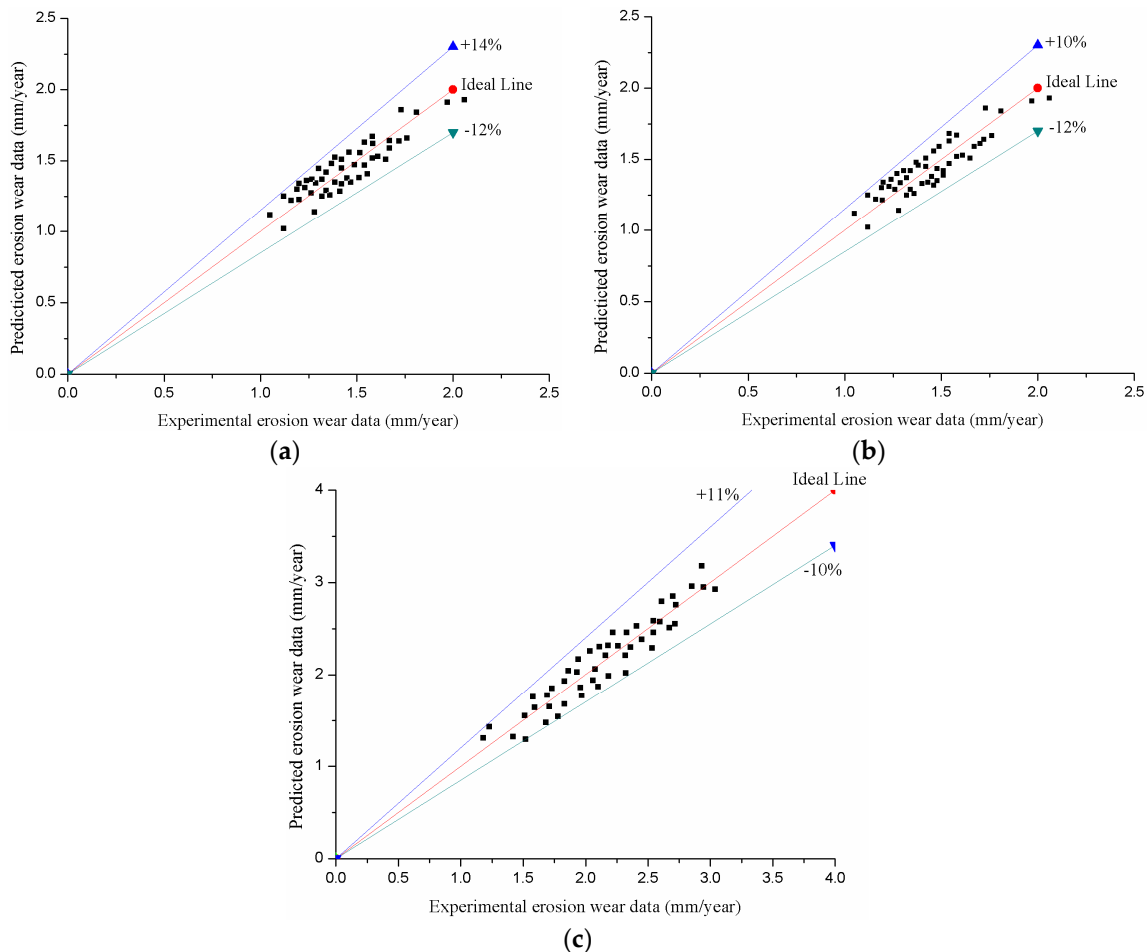


Figure 9. Variation of erosion wear for experimental and theoretical values: (a) mild steel; (b) SS202 and (c) SS304.

4. Conclusions

Present study was conducted with the motivation of measuring average erosion wear on specimens placed in a horizontal direction. The erosion wear on three different slurry pipe materials, namely, mild steel, SS202 and SS304 due to slurry mixture flow has been investigated using a slurry erosion pot tester. Erosion tests were conducted to establish the influence of rotational speed, concentration, and time period. On the basis of the experimental investigation, the following concise and precise forms of outcomes are found: SS202 shows better erosion resistance as compared with mild steel and SS304 under all circumstances. Rotational speed is found to be a highly influencing parameter for the erosion wear rate as compared to solid concentration, time duration, and weighted mean diameter. WC- $_{10}$ Co $_4$ Cr HVOF coating improved the erosion resistance of piping materials up to 3.5 times. The predicted erosion wear is in agreement with the experimental data and found within a deviation of $\pm 12\%$.

Acknowledgments: The authors would like to inform that this work did not receive any grant from any funding agency either from public or commercial sector.

Author Contributions: Kaushal Kumar and Satish Kumar conceived and designed the experiments; Kaushal Kumar and Gurprit Singh performed the experiments; Kaushal Kumar, Jashanpreet Singh and Jatinder Pal Singh analyzed the data; Kaushal Kumar and Jashanpreet Singh wrote the paper; Satish Kumar supervised the whole work. All the authors have read and approved the final manuscript.

Conflicts of Interest: The authors declare no conflict of interest.

References

1. Kumar, S.; Mohapatra, S.K.; Gandhi, B.K. Effect of addition of fly ash and drag reducing on the rheological properties of bottom ash. *Int. J. Mech. Mater. Eng.* **2013**, *8*, 1–8.
2. Gandhi, B.K.; Singh, S.N.; Seshadri, V. Study of the parametric dependence of erosion wear for the parallel flow of solid–liquid mixtures. *Tribol. Int.* **1999**, *32*, 275–282. [[CrossRef](#)]
3. Gandhi, B.K.; Singh, S.N.; Seshadri, V. A study on the effect of surface orientation on erosion wear of flat specimens moving in a solid-liquid suspension. *Wear* **2003**, *254*, 1233–1238. [[CrossRef](#)]
4. Chandel, S.; Singh, S.N.; Seshadri, V. An experimental study of erosion wear in a centrifugal slurry pump using coriolis wear test rig. *Particul. Sci. Technol.* **2012**, *30*, 179–195. [[CrossRef](#)]
5. Kosa, E.; Göksenli, A. Effect of impact angle on erosive abrasive wear of ductile and brittle materials. *Int. J. Mech. Aerosp. Ind. Mechatron. Manuf. Eng.* **2015**, *9*, 1638–1642.
6. Modi, O.P.; Dasgupta, R.; Prasad, B.K. Erosion of a high carbon steel in coal and bottom ash slurries. *J. Mater. Eng. Perform.* **2000**, *9*, 522–529. [[CrossRef](#)]
7. Desale, G.R.; Gandhi, B.K.; Jain, S.C. Slurry erosion of ductile materials under normal impact condition. *Wear* **2008**, *264*, 322–330. [[CrossRef](#)]
8. Prasad, B.K.; Jha, A.K.; Modi, O.P. Effect of sand concentration in the medium and travel distance and speed on the slurry wear response of a zinc-based alloy alumina particle composite. *Tribol. Lett.* **2004**, *17*, 301–309. [[CrossRef](#)]
9. Shitole, P.P.; Gawande, S.H.; Desale, G.R. Effect of impacting particle kinetic energy on slurry erosion wear. *J. Bio-Tribo-Corros.* **2015**, *1*, 29. [[CrossRef](#)]
10. Kulu, P.; Käerdi, H.; Surzenkov, A. Recycled hard metal-based powder composite coatings: Optimisation of composition, structure and properties. *Int. J. Mater. Prod. Technol.* **2014**, *49*, 180–202. [[CrossRef](#)]
11. Xie, Y.; Pei, X.; Wei, S. Investigation of erosion resistance property of WC-Co coatings. *Int. J. Surf. Sci. Eng.* **2016**, *10*, 365–374. [[CrossRef](#)]
12. Cho, T.Y.; Yoon, J.H.; Kim, K.S. A study on HVOF coatings of micron and nano WC-Co powders. *Surf. Coat. Technol.* **2008**, *202*, 5556–5559. [[CrossRef](#)]
13. Ma, H.R.; Li, J.W.; Jiao, J. Wear resistance of Fe-based amorphous coatings prepared by AC-HVAF and HVOF. *Mater. Sci. Technol.* **2017**, *33*, 65–71. [[CrossRef](#)]
14. Valentinelli, L.; Valente, T.; Casadei, F. Mechanical and tribocorrosion properties of HVOF sprayed WC–CO coatings. *Corros. Eng. Sci. Technol.* **2004**, *39*, 301–307. [[CrossRef](#)]
15. Gupta, R.; Singh, S.N.; Seshadri, V. Prediction of uneven wear in a slurry pipeline on the basis of measurements in a pot tester. *Wear* **1995**, *184*, 169–178. [[CrossRef](#)]
16. Desale, G.R.; Gandhi, B.K.; Jain, S.C. Improvement in the design of a pot tester to simulate erosion wear due to solid–liquid mixture. *Wear* **2005**, *259*, 196–202. [[CrossRef](#)]
17. Goyal, D.K.; Singh, H.; Kumar, H.; Sahni, V. Slurry erosion behavior of HVOF sprayed WC–₁₀Co₄Cr and Al₂O₃ + 13TiO₂ coatings on a turbine steel. *Wear* **2012**, *289*, 46–57. [[CrossRef](#)]
18. Truscott, G.F. *A Literature Survey on Wear on Pipelines*; Publication TN 1295; BHRA Fluid Engineering: Cranfield, UK, 1975.
19. Bajracharya, T.R.; Acharya, B.; Joshi, C.B.; Saini, R.P.; Dahlhaug, O.G. Sand erosion of Pelton turbine nozzles and buckets: A case study of Chilime hydropower plant. *Wear* **2008**, *264*, 177–184. [[CrossRef](#)]

